Durability Analysis and Structural Health Management of Smart Composite Structures Using Small-Diameter Fiber Optic Sensors

N. Takeda* and Y. Okabe

Department of Advanced Energy, Graduate School of Frontier Sciences, The University of Tokyo and Department of Aeronautics and Astronautics, School of Engineering, The University of Tokyo

ABSTRACT

The authors and Hitachi Cable, Ltd. have recently developed small-diameter optical fiber sensors in order to embed the sensors inside a lamina of composite laminates without strength reduction. The outside diameters of the cladding and polyimide coating are 40 and 52 μm, respectively. This paper presents a summary of applications of the small-diameter optical fiber sensors to damage monitoring in composite structures. First, small-diameter fiber Bragg grating (FBG) sensors were applied to detect transverse cracks and delamination in CFRP cross-ply laminates using the changes in the form of the reflection spectrum. The same monitoring technique was extended to detect both free-edge and impact-induced delaminations in CFRP quasi-isotropic laminates. The sensors also detected the debonding of CFRP repair patches from an aluminum structure. Small-diameter FBG sensors were also successfully used to monitor the thermal residual stress during the fabrication process. Then, the multi-mode damage pattern of a notched cross-ply laminates was identified as an inverse problem using the reflection spectrum as an objective function. Furthermore, applications of small-diameter optical fibers and FBG sensors were demonstrated in a stiffened CFRP fuselage structure of 1.5 m in diameter and 3 m in length. The small-diameter optical fiber sensors were successfully embedded into the upper panel of the fuselage, and the real-time detection system could well detect impact locations and impact-induced damages.

Key words: structural health monitoring, durability, small-diameter optical fiber, fiber Bragg grating sensor, reflection spectrum, delamination, transverse cracks

1. INTRODUCTION

In recent years, structural health monitoring technologies for composite structures have been studied extensively in order to assess the safety and the durability of the structures. A potential candidate for the sensing device is an optical fiber Bragg grating (FBG) sensor /1/. FBG sensors are very sensitive to non-uniform strain distribution along the entire length of the grating, which deforms the reflection spectrum from the FBG sensors. Taking advantage of the sensitivity, microscopic damages that cause non-uniform strain distribution in CFRP laminates can be detected. In order to embed the sensors into the laminates near the critical location where the damages might occur without introducing any defects and strength reduction, the authors and Hitachi Cable, Ltd. developed small-

* Author to whom all correspondence should be addressed:
Nobuo Takeda, Department of Advanced Energy, Graduate School of Frontier Sciences, The University of Tokyo, Mail Box 302, 5-1-5 Kashiwanoha, Kashiwa-City, Chiba 277-8561, Japan
E-mail: takeda@smart.k.u-tokyo.ac.jp

diameter optical fibers and their FBG sensors whose coating outside diameter is 52 µm /2/.

In this study, the small-diameter FBG sensors were applied to detect transverse cracks and delaminations in CFRP cross-ply and general quasi-isotropic laminates in different loading conditions, and debond growth in composite repair patches. The monitoring of the thermal residual stress during the fabrication process was also conducted. A method for the multi-mode damage pattern identification was also proposed as an inverse problem using the reflection spectrum. Then, the small-diameter optical fibers and FBG sensors were embedded in a stiffened CFRP fuselage structure of 1.5 m in diameter and 3 m in length and applied to detect impact-induced damages in the demonstration structure.

2. DEVELOPMENT OF SMALL-DIAMETER OPTICAL FIBERS AND FBG SENSORS AND APPLICATION TO DAMAGE DETECTION

2-1. Development of small-diameter optical fibers and FBG sensors

The small diameter optical fibers (both single-mode and multi-mode) were developed and FBG sensors were fabricated with these optical fibers (Fig. 1). The optical fiber is with 40 µm in cladding diameter and 52 µm in polyimide coating diameter, which is easily embedded within one CFRP ply of typically 125 µm in thickness. Such optical fibers have both mechanical and optical properties similar to those of conventional optical fibers with 125 µm in cladding diameter and do not cause any reduction in strength of composites when embedded parallel to reinforcing fibers in laminates /2/. When a small-diameter optical fiber is embedded inside a lamina, resin-rich regions cannot be found around the fiber, as shown in Fig. 2. The polyimide coating relieves the stress concentration around the cladding with a proper combination of the stiffness and the thickness. The coating is also highly compatible with epoxy or other high-temperature polymer matrix of CFRP composites under high-temperature exposure during fabrication and also in high-temperature use.

Then, FBG sensors were also successfully developed with these single-mode small-diameter optical fibers, where periodic gratings with approximately 0.53 µm in space were inscribed in the gage section (typically 10 mm in length). When a broadband light is introduced from one end of the fiber, a narrow-band spectrum with a sharp wavelength peak corresponding to the grating spacing is obtained if uniform strain within the gage section can be assumed. FBG sensors are usually used to measure strain and/or temperature through the shift of the wavelength peak /1/.

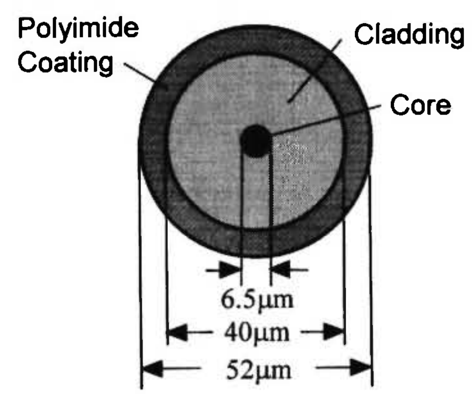

Fig. 1: Small-diameter optical fiber

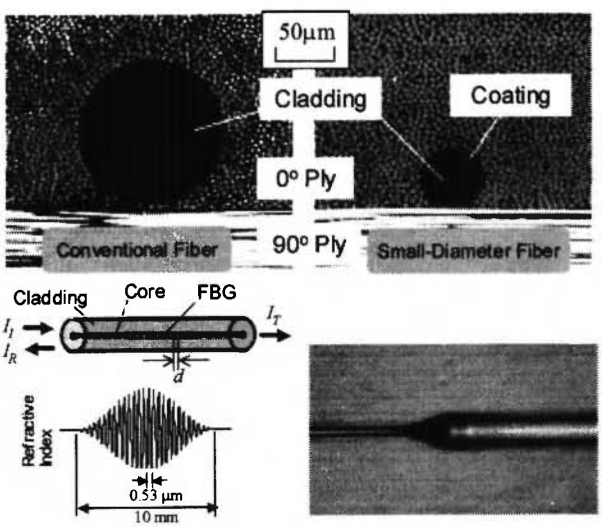

Fig.2: Conventional and small-diameter optical fibers embedded in a CFRP lamina and small-diameter FBG sensors with fiber connection to conventional optical fiber.

2-2. Detection of transverse cracks by embedded small-diameter FBG sensors

Although the peak shift phenomenon due to the axial strain or the temperature change is normally used as a sensing mechanism of FBG sensors, they are very sensitive to non-uniform strain distribution along the entire length of the grating (Fig. 3). The small-diameter optical fibers enable us to embed the FBG gage section near the location where the damages might occur in the laminate. Then, the strain distribution due to microscopic damages sensitively deforms the reflection spectrum from the FBG sensors. This sensitivity can be used to detect microscopic damages in CFRP /3-6/. After the monitoring methodology was established for cross-ply laminates /3, 4/, transverse cracks were monitored in general quasi-isotropic laminates /5/.

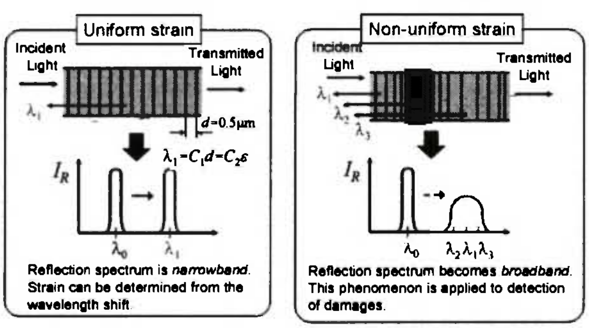

Fig. 3: Response of FBG sensors to uni-form and non-uniform strain dis:ribution

When an FBG sensor was embedded in the -45° ply to detect transverse cracks in the adjacent 90° ply of CFRP quasi-isotropic laminate $[45/0/\text{-}45/90]_s$ (Fig. 4), a non-uniform strain distribution due to the initiation and evolution of transverse cracks caused the wavelength distribution in the reflected light, as shown in Fig. 5 /5/. While there were no transverse cracks, the spectrum kept its shape and the center wavelength shifted corresponding to the applied strain. With increasing transverse crack density, the shape of the reflection spectrum was distorted; the intensity of the highest peak became small, some peaks appeared around it, and the spectrum became broad. These experimental observations could be well explained by the theoretical prediction using the calculated strain distribution and the fiber optic theory /3-6/. The location of transverse cracks could be also obtained when a chirped FBG sensor with gradual change in grating period along the gage length was used /6/. The crack location can be well correlated with the wavelength in the spectrum.

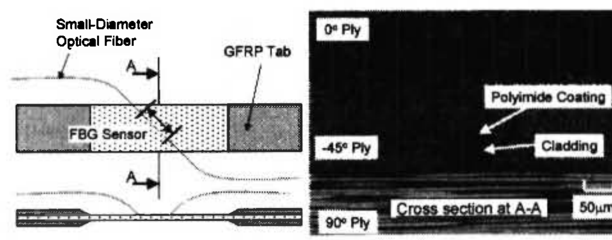

Fig. 4: A small-diameter FBG sensor embedded in the $-45°$ ply for detection of transverse cracks in the adjacent 90° ply of quasi-isotropic $/45/0/\text{-}45/90/_s$ laminate.

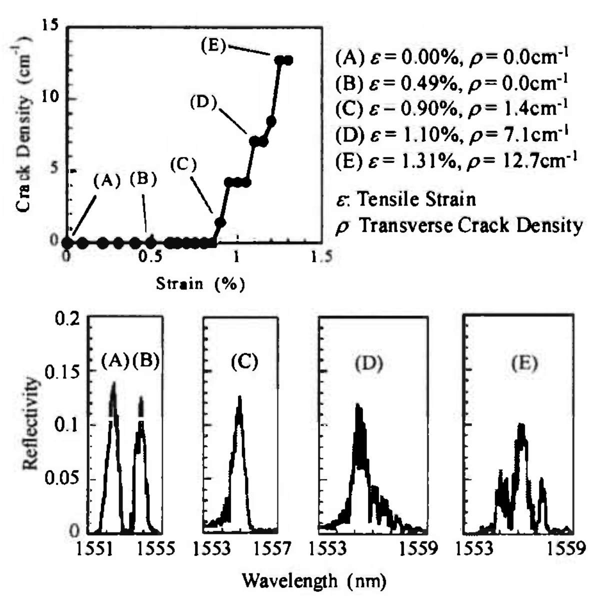

Fig. 5: Change in wavelength distribution of reflected light from the FBG sensor due to the evolution of transverse cracks.

2-3. Detection of delamination by embedded small-diameter FBG sensors

2-3-1. Delamination in four-point flexural tests

The same principal can be applied to the detection of delamination, which is the most important damage for structural design of composite laminates. Figure 6 shows the quantitative measurement results of delamination growth in four-point flexural tests for cross-ply laminates /7/. The two peaks at shorter and longer wavelengths in the reflection spectrum correspond to the strain levels of the bonded and delaminated areas, respectively (Fig. 7). The intensity ratio of the two peaks is a quantitative parameter for the delamination growth (Fig. 8). The theoretical prediction using the calculated strain distribution by finite element (FE) analysis and the fiber optic theory was also found to agree well with the experiments /7/.

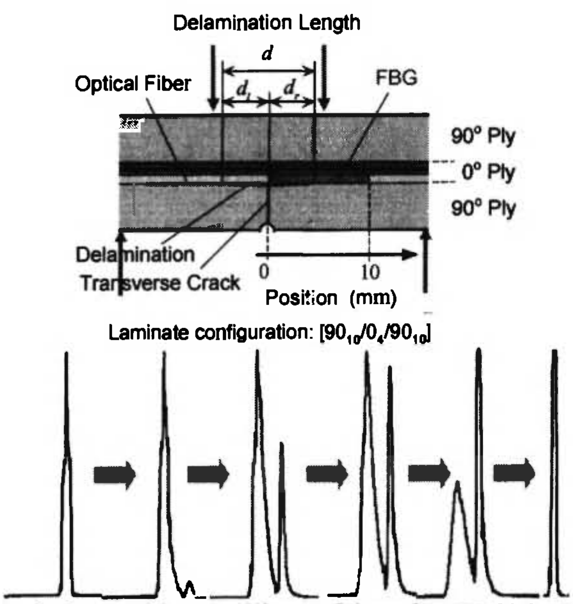

Fig. 6: Quantitative measurement of the reflection spectrum during the delamination growth in four-point flexural tests for cross-ply laminates.

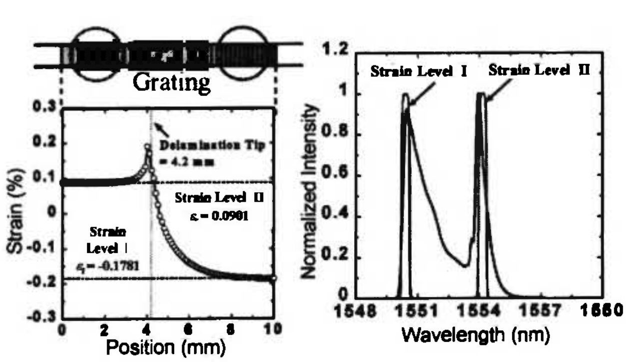

Fig. 7: Strain distribution and calculated reflection spectrum. The two peaks at shorter and longer wavelengths correspond to the strain levels of the bonded and delaminated areas, respectively.

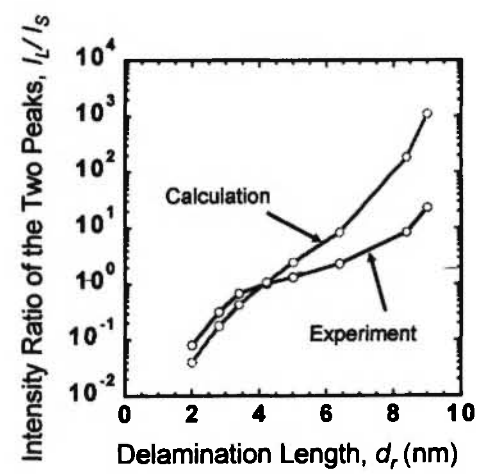

Fig. 8: Intensity ratio of the two peaks as a quantitative parameter for the delamination growth

2-3-2. Free-edge delamination

Figures 9 and 10 show the specimen with an embedded FBG sensor and the experimental results for detection of free-edge delamination of CFRP /45/-45/0/90/$_s$ laminate /8/. It should be noted that small-diameter optical fibers can be embedded and taken out of the laminate without introducing any significant defect. The free-edge delamination grew alternatively at 0/90 and 90/90 interfaces under tension-tension fatigue loading. An initial single peak in the reflection spectrum was separated into two peaks, and the peak at longer wavelength grew as the edge delamination grew. This change in the reflection spectrum was found to be well predicted by the theoretical prediction /8/. This technique can be also applied to other types of delamination detection around stress-concentrated regions such as rivet holes.

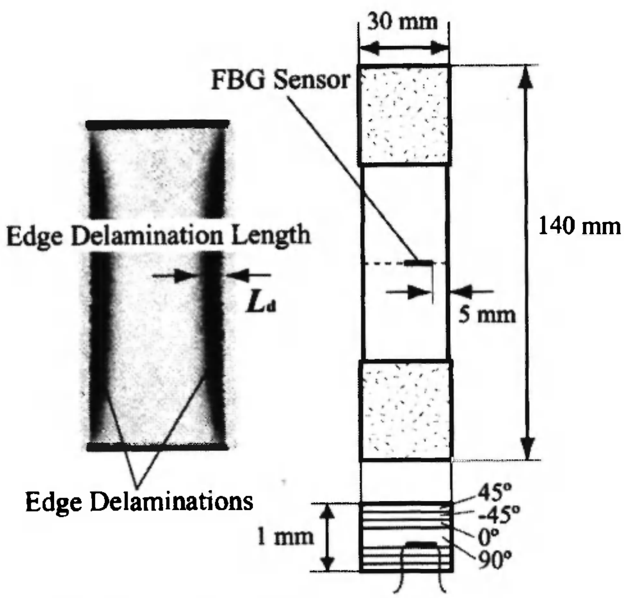

Fig. 9: Schematic of $[45/-45/0/90]_s$ edge delamination specimen with an embedded FBG sensor.

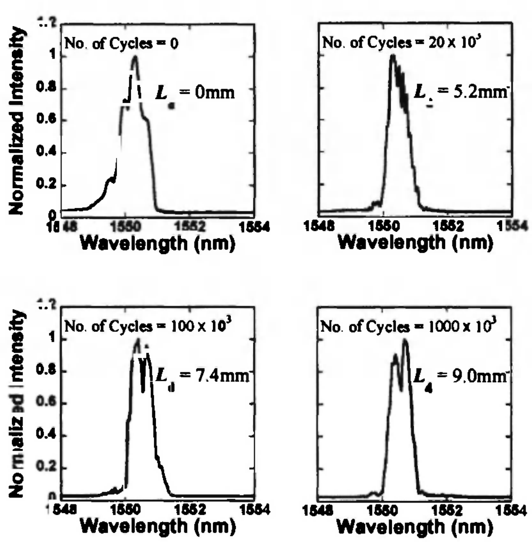

Fig. 10: Change in wavelength distribution of reflected light from the FBG sensor due to the edge delamination growth.

2-3-3. Impact-induced delamination

Low-velocity transverse impact often induces delaminations and matrix cracks in CFRP laminates, which are barely visible from the outer surface. For practical use of the CFRP laminates, it is important to monitor the impact damage state. The transverse impact loading was applied to the cross-ply $[0_4/90_4/0_4]$ specimen ($100 \times 100 \times 1.5$ mm^3) with a drop-weight impact tester. The applied impact energy levels were 1.0J, 2.0J, and 3.0J. Typical damages in the laminate were two peanut-shape delaminations at upper and lower 0°/90° interfaces, shear cracks in 90° ply, and a bending crack in lower 0° ply (Fig. 11). The small-diameter FBG sensor was embedded into 90° ply in contact with the lower 0°/90° interface in order to detect the delamination at the lower interface. The reflection spectrum from the embedded FBG was measured using the optical spectrum analyzer after the impact test to observe any change /9/.

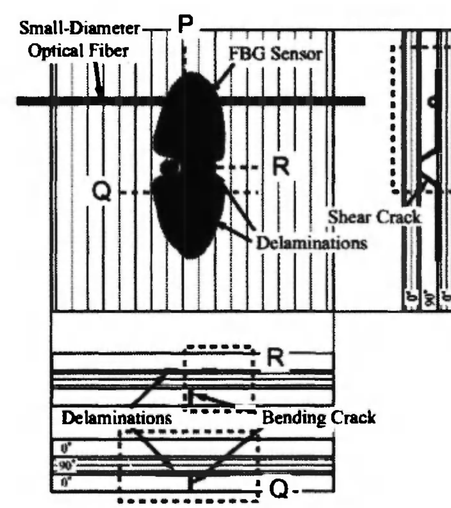

Fig. 11: Schematic view of specimen configuration and impact-induced damages in the cross-ply laminate.

Figure 12 shows photographs of the lower 0°/90° interfacial delamination observed by ultrasonic C-scan. The size of the delamination increased with an increase in the impact energy level. A bending crack appeared in all the pictures. The reflection spectra measured before and after the impact tests are shown in Fig. 12. These are normalized by the intensity of the highest component. When the impact energy was 1.0J, the delamination did not reach to the FBG sensor and the bending crack passed under the sensor. In this case, the reflection spectrum was deformed drastically. At the impact energy of 2.0J, the tip of the delamination passed

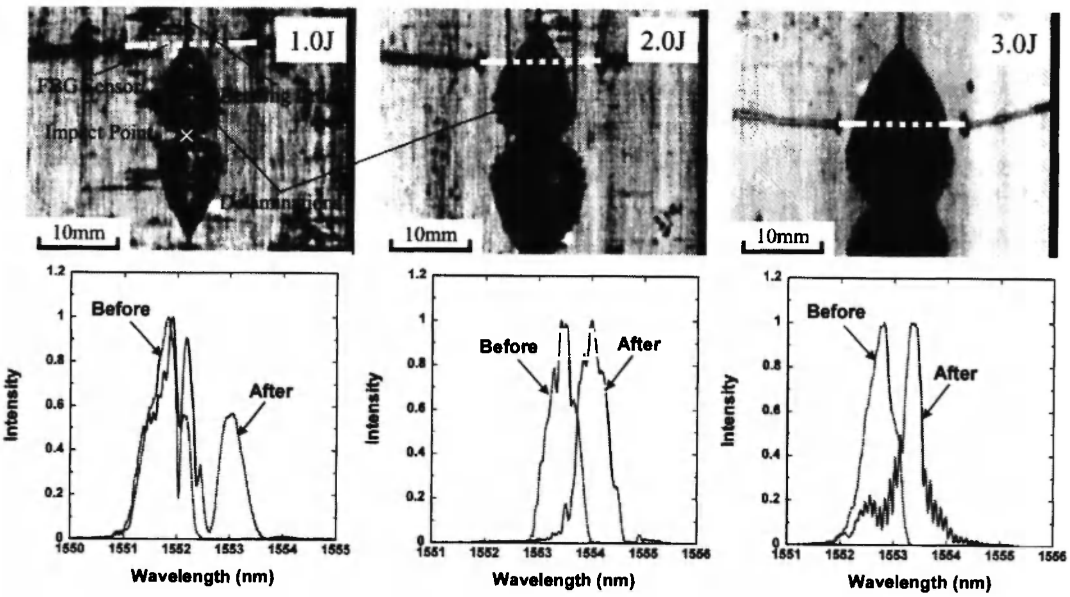

Fig. 12: Photographs of the lower 0°/90° interfacial delamination observed by ultrasonic C-scan and the corresponding reflection spectra.

through the FBG sensor, and the reflection spectrum had one large peak at the longer wavelength and some small components at the shorter wavelength. Then, when the impact energy was increased to 3.0J, the delamination covered the entire gauge length of the FBG sensor, and the reflection spectrum shifted its center wavelength without the deformation.

*2-3-4. **Debonding of composite patches***

Moreover, this technique was applied for the detection of cyclic debond growth in composite repair patches /10/. The patch was CFRP unidirectional laminate $[0]_4$ and was glued on both sides of an aluminum plate using adhesive films AF-163-2K (Fig. 13). The small-diameter FBG sensor was embedded into the adhesive layer in contact with the CFRP patch. When cyclic tensile load was applied to the repaired aluminum plate, delaminations appeared between the adhesive and the aluminum plate from the ends of the adhesive layer and progressed along the loading direction. Similarly, two peaks appeared in the reflection spectrum and the intensity ratio of the two peaks changed depending on the debonding length as shown in Fig. 14.

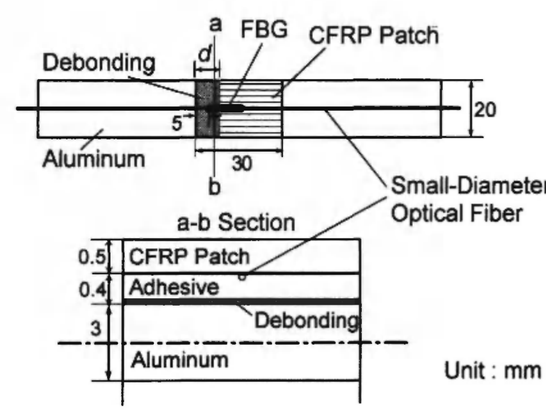

Fig.13: CFRP repair patch adhered on aluminum plate with a small-diameter FBG sensor embedded in the adhesive layer.

2.4. Multiple-mode damage identification using the reflection spectrum

So far, we have noticed that the reflection spectrum of an FBG sensor is useful for monitoring the damage pattern, because it contains much information on the strain distribution within the gage section. Here, we attempt to identify the damage pattern of a notched cross-ply composite laminate as an inverse problem using a reflection spectrum of an embedded FBG sensor /11/.

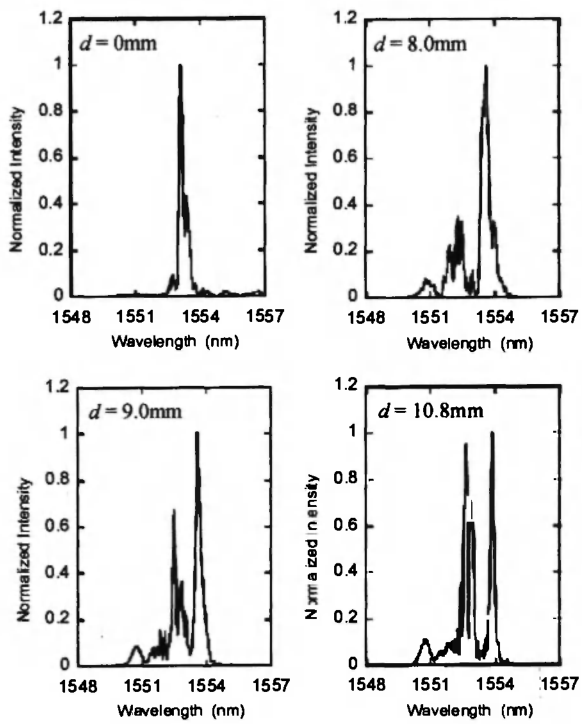

Fig. 14: Change in wavelength distribution of reflected light from the FBG sensor due to the debonding of the CFRP patch.

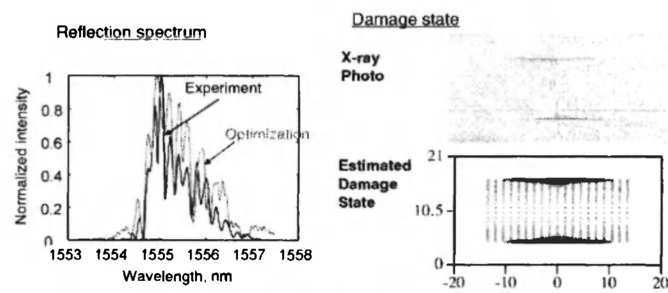

		Experiment	Identification
Splitting		7.4	7.8~9.1
Delamination	major axis	2.7	3.4~7.8
	minor axis	1.0	0.9~2.0
Transverse cracks		6 cracks	4 cracks

Fig. 15: Estimation of the damage pattern of a notched cross-ply composite laminate as an inverse problem using a reflection spectrum of an embedded FBG sensor.

The damage pattern near the notch includes multi-mode damages: splits in 0-degree ply, transverse cracks in 90-degree ply and delamination at 0/90 interfaces as shown in Fig. 15. The evolution of such damage pattern was modeled using layer-wise FE analysis with cohesive elements to represent various cracks (Fig. 16). Then, the reflection spectrum was predicted by combining the FE-calculated strain distribution and the fiber optic theory. Based on the above forward analysis, the damage pattern represented by the design variables such as transverse crack density, delamination length and split length and so on., was optimized as an inverse problem while the spectrum shape was adopted as the objective function. In the estimation scheme, the damage pattern was expressed using the residual strength distribution of cohesive elements depending on the design variables. The identified damage pattern agreed well with the experimental one (Fig. 15).

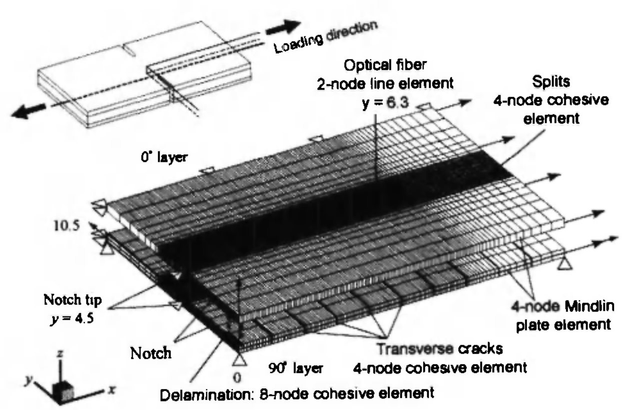

Fig. 16: Model for layer-wise FE analysis with cohesive elements to represent various cracks

2.5. Monitoring of thermal residual stresses during fabrication process by embedded small-diameter FBG sensors

FBG sensors can monitor the axial thermal residual stress during the fabrication process. However, the reflection spectra are normally deformed just after the fabrication of the laminates, because of non-axisymmetric thermal residual stresses due to the embedment. This deformation of the spectrum will lead to misreading in the measurement. In order to study the effect of the thermal residual stress, the reflection spectrum was measured during the fabrication process of the laminates /12, 13/. Figure 17 shows the comparison between the experiment and the theoretical prediction considering the birefringence effect due non-axisymmetric thermal residual stresses introduced during the fabrication. This result suggests that FBG sensors are very useful in both fabrication monitoring and damage monitoring.

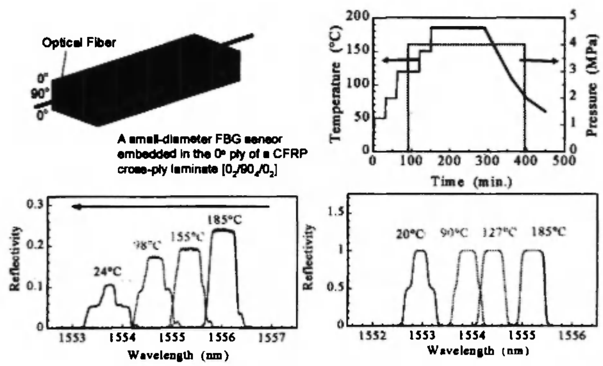

Fig. 17: Monitoring of thermal residual stresses during fabrication process by embedded small-diameter FBG sensors

In addition, the following fundamental studies were also conducted for applications of small-diameter FBG sensors: (1) effects of coating on the damage detection by FBG sensors /14/, (2) temperature-compensated strain measurement sensor using an FBG sensor /15/, and (3) a combined damage monitoring and suppression system of CFRP laminates using FBG sensors and SMA (shape memory alloy) foil actuators /16/.

3. DAMAGE DETECTION IN COMPOSITE STIFFENED FUSELAGE STRUCTURE

In the "R&D for Smart Material/Structure System (SMSS)" project (October 1998 to March 2003) as one of the Academic Institutions Centered Program supported by NEDO (New Energy and Industrial Technology Development Organization) Japan, two demonstrators were manufactured. One was aimed at Damage Detection and Suppression, and the other was at Noise and Vibration Reduction. These were cylindrical fuselages made of composite structures, whose length was 3 m and diameter was 1.5 m /17/.

The Damage Detection and Suppression Demonstrator (Fig. 18) was rigidly supported at one end

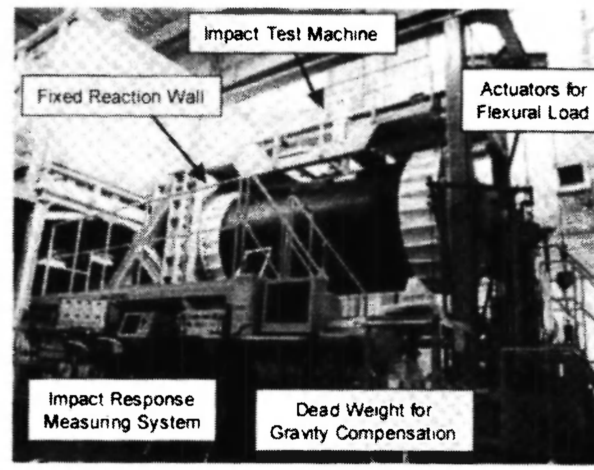

Fig. 18: Final assembly of the Damage Detection and Suppression Demonstrator

and subjected to the upward shear load up to approximately 240 kN at the other end by hydraulic actuators, resulting in approximately 3,600 $\mu\varepsilon$ strain at maximum at the gage section of both upper and lower panels. The internal pressure up to 75 kPa was also applied in the pressurization stage. Several load-unload cycles were applied to the Demonstrator in order to measure the response of the structure under loading and to confirm the repeatability of the data. The following six themes were selected for demonstration (Fig. 19): (1) real time detection of impact damage with embedded small-diameter optical fiber sensors, (2) real time impact detection with integrated acoustic emission sensor network system, (3) strain distribution measurement using distributed BOTDR (Brillion Optical Time Domain Reflectmetry) technique, (4) damage suppression using embedded SMA foils, (5) maximum strain memory sensors by electric conductivity change in CFRP patch, and (6) smart manufacturing of low-cost sensor integrated panel by resin transfer molding.

Development of real time detection of impact damage with embedded small-diameter optical fiber

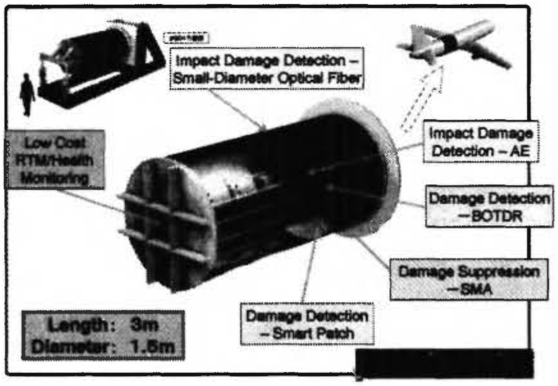

Fig. 19: Selected themes in Damage Detection and Suppression Demonstrator Test

sensors was conducted as a collaborative work between the University of Tokyo and Kawasaki Heavy Industries. Monitoring of the impact load on composite laminates was successfully made with embedded multi-mode small-diameter optical fibers /18, 19/. The bending loss was observed only during impact loading. The maximum magnitude of optical loss was found to be proportional to that of the impact load. Several small-diameter FBG sensors were also used to obtain the impact location through the dynamic strain measurement. Figure 20 shows the impact test specimens from flat coupons to stiffened flat and curved panels with embedded small-diameter optical fibers.

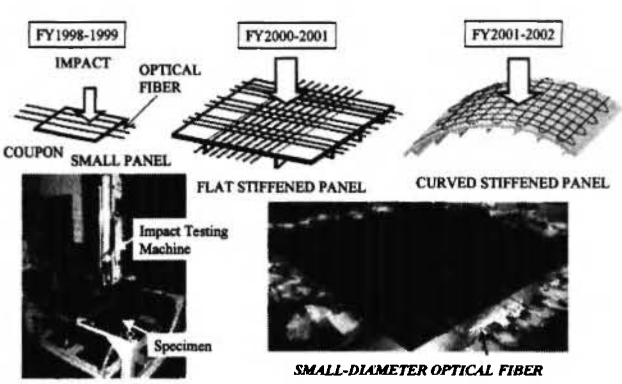

Fig. 20: Impact test specimens from coupons to stiffened flat and curved panels with embedded small-diameter optical fibers

In the upper panel of the Damage Detection and Suppression Demonstrator in Fig. 18, the small-diameter optical fiber sensors were embedded in order to detect impact-induced damages (Fig. 21) /20/. The fiber connecters had been well designed to be embedded so that the fabricated CFRP panel could be trimmed at the edges after the manufacturing for practical use (Fig. 22). The small-diameter FBG sensors were used to

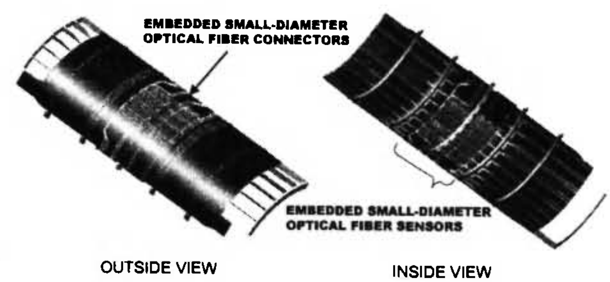

Fig.21: Schematic of arrangement of embedded small-diameter optical fibers in the upper panel.

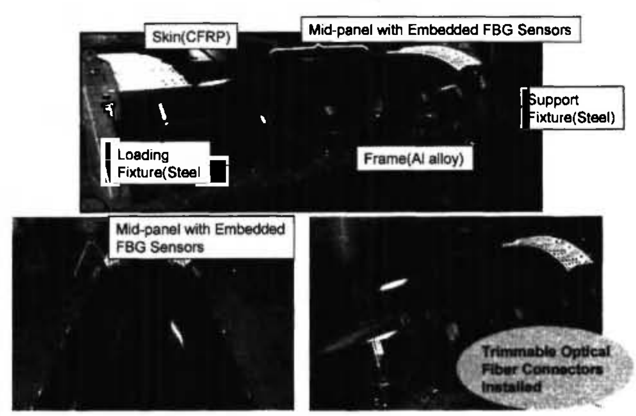

Fig. 22: Upper panel with embedded small-diameter optical fibers and trimmable connectors.

obtain the impact location through the dynamic strain measurement, and multi-mode small-diameter optical fibers were embedded to judge the occurrence of the impact-induced damages using the optical loss due to bending. The algorism of impact load and damage evaluation and visualization system is shown in Fig. 23. Then, a novel impact detection and localization system was also developed as shown in Figure 24. This system could successfully detect the impact locations and impact-induced damages.

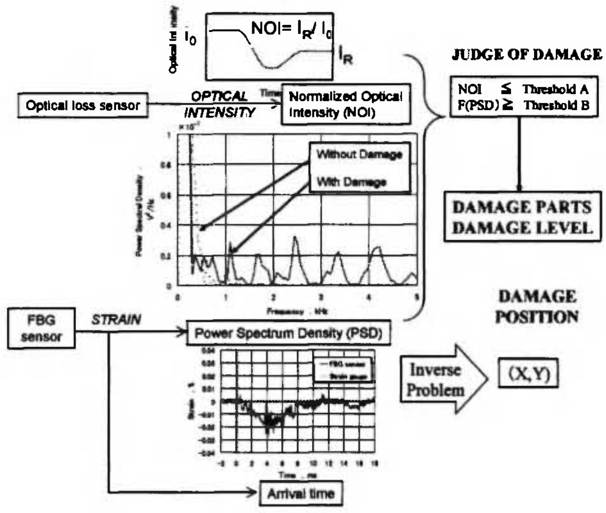

Fig. 23: Algorism of impact load and damage evaluation/visualization system

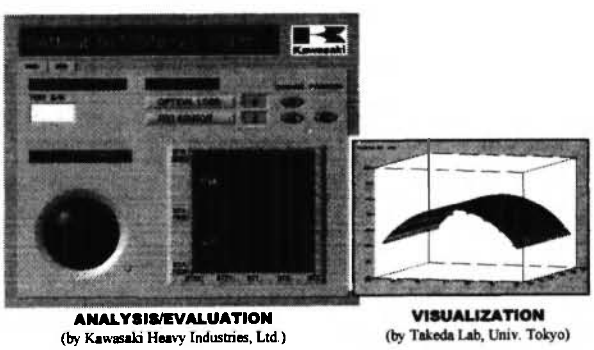

Fig. 24: A developed impact detection and localization system. The system judged a delamination at the impact region.

The authors are also applying small-diameter FBG sensors to other composite structures. Fabrication and damage monitoring procedure was demonstrated in CFRP space satellite panel structures /21/. Real time strain monitoring of composite LH_2 cryogenic tank during the flight operation was successfully conducted using a developed onboard FBG demodulator mounted on a reusable launch vehicle /22/. Detection of transverse cracks was also attempted in the pressurization test. Lamb waves in composite laminates were also detected using a developed high-speed demodulation system and used to detect the debond growth in bonded composite stiffened panel structures /23, 24/.

4. CONCLUSIONS

In this study, small-diameter FBG sensors were applied to detect damages in CFRP laminates. From the changes in the form of the reflection spectrum, transverse cracks and various types of delaminations in CFRP quasi-isotropic laminates could be well evaluated. The sensors also detected the debonding of CFRP repair patches from an aluminum structure and measured the thermal residual stresses during the fabrication process. Then, a damage identification method was proposed for multi-mode damage as an inverse problem using the FBG reflection spectrum. Furthermore, the small-diameter optical fibers and FBG sensors were embedded into the CFRP cylindrical fuselage. The developed monitoring system could detect the impact locations and impact-induced damages successfully.

ACKNOWLEGDEMENTS

Small-diameter optical fiber and FBG sensors were developed in the "R&D for Smart Material/Structure System" project (1998-2003) within the Academic Institutions Centered Program supported by New Energy and Industrial Technology Development Organization (NEDO), Japan. The authors deeply acknowledge the support of the participating members in the project for their research efforts. They also thank Dr. A. Hongo, Dr. Y. Kurosawa, Mr. K. Fukuchi, Mr. S. Kojima, and Mr. K. Satori of Hitachi Cable, Ltd. for continuing collaboration. Special thanks are also extended to Mr. T. Sakurai, Mr. N. Tajima and Mr. M. Sasajima of RIMCOF (R&D Res. Inst. for Metals and Composites for Future Industries) for the project management.

REFERENCES

1. A.D. Kersey, M.A. Davis, H.J. Patrick, M. LeBlanc, K.P. Koo, C.G. Askins, M.A.Putnam, and E.J. Friebele, Fiber grating sensors, *Journal of Lightwave Technol.*, **15**(8), 1442-1463 (1997).
2. K. Satori, K. Fukuchi, Y. Kurosawa, A. Hongo and

N. Takeda, Polyimide-coated small-diameter optical fiber sensors for embedding in composite laminate structures, *Proc. SPIE*, Vol. 4328, 285-294. Bellingham: SPIE (2001).

3. Y. Okabe, S. Yashiro, T. Kosaka and N. Takeda, Detection of transverse cracks in CFRP composites using embedded fiber Bragg grating sensors, *Smart Mater. Struct.*, 9(6), 832-838 (2000).
4. Y. Okabe, T. Mizutani, S. Yashiro and N. Takeda, Detection of microscopic damages in composite laminates with embedded small-diameter fiber Bragg grating sensors, *Comp. Sci. Technol.*, **62**, 951-958 (2002).
5. T. Mizutani, Y. Okabe and N. Takeda, Quantitative evaluation of transverse cracks in carbon fiber reinforced plastic quasi-isotropic laminates with embedded small-diameter fiber Bragg grating sensors. *Smart Mater. Struct.*, **12**(6), 898-903 (2003).
6. Y. Okabe, R. Tsuji and N. Takeda, Application of chirped fiber Bragg grating sensors for identification of crack locations in composites, *Composites Part A*, **35** , 59-65 (2004).
7. S. Takeda, Y. Okabe and N. Takeda, Delamination detection in CFRP laminates with embedded small-diameter fiber Bragg grating sensors, *Composites Part A*, **33**, 971-980 (2002).
8. S. Takeda, Y. Okabe, T. Yamamoto and N. Takeda, Detection of edge delamination in CFRP laminates under cyclic loading using small-diameter FBG sensors. *Comp. Sci. Tech.*, **63**(13), 1885-1894 (2003).
9. S. Minakuchi, S. Takeda, Y. Okabe and N. Takeda, Detection of impact damages in CFRP cross-ply laminates using small-diameter FBG sensors, *Proc. 8th Japan Inter. SAMPE Symp.*, 261-264 (2003).
10. T. Yamamoto, S. Takeda, Y. Okabe and N. Takeda, Health monitoring of a bonded repair patch using small-diameter FBG sensors, *Proc. 8th Japan Inter. SAMPE Symp.*, 159-162 (2003).
11. S. Yashiro, N. Takeda. T. Okabe and H. Sekine, A new approach to predicting multiple damage states in composite laminates with embedded FBG sensors, *Comp. Sci. Technol.* (accepted for publication).
12. Y. Okabe, S. Yashiro, R. Tsuji, T. Mizutani and N. Takeda, Effects of thermal residual stress on the reflection spectrum from fiber Bragg grating sensors embedded in CFRP laminates, *Composites Part A*, **33**, 991-999 (2002).
13. Y. Okabe, R. Tsuji and N. Takeda, Measurement of transverse thermal residual strain in CFRP laminates using FBG sensors, *Proc. 8th Japan Inter. SAMPE Symp.,* 171-174 (2003).
14. Y. Okabe, N. Tanaka and N. Takeda, Effect of fiber coating on crack detection in carbon fiber reinforced plastic composites using fiber Bragg grating sensors, *Smart Mater. Struct.*, **11**, 892-898 (2002).
15. N. Tanaka, Y. Okabe and N. Takeda, Temperature-compensated strain measurement using fiber Bragg grating sensors embedded in composite laminates, *Smart Mater. Struct.*, **12**, 940-946 (2003).
16. I. Taketa, M. Amano, Y. Okabe and N. Takeda, Damage detection and suppression system of CFRP laminates with FBG sensor and SMA actuator, *Trans. Mater. Res. Soc. Japan*, **28**(3), 675-678 (2003).
17. N. Tajima, T. Sakurai, M. Sasajima, N. Takeda, and T. Kishi, Overview of the demonstrator program in Japanese smart material and structure system project, *Adv. Comp. Mater.*, **13**(3), 3-5 (2004).
18. H. Tsutsui, A. Kawamata, T. Sanda and N. Takeda, Impact damage monitoring of composite panels by embedded small-diameter optical fibers, *Mater. Sci. Res. Inter., Spec. Tech. Pub.* Part 2, 121-125 (2001).
19. H. Tsutsui, A. Kawamata, T. Sanda and N. Takeda, Detection of impact damage of stiffened composite panels using embedded small-diameter optical fibers, *Smart Mater. Struct.*, **13**, 1284-1290 (2004).
20. H. Tsutsui, A. Kawamata, J. Kimoto, A. Isoe, Y. Hirose, T. Sanda and N. Takeda, Impact damage detection system using small-diameter optical fiber sensors embedded in CFRP laminate structures, *Adv. Comp. Mater.*, **13**(3), 3-5 (2004).
21. H. Takeya, S. Kabashima, T. Ozaki and N. Takeda, Monitoring of a structural panel for space satellite using FBG sensor, *Proc. First Euro.*

Workshop Struct. Health Monitoring, 919-925 (2002).

22. T. Mizutani, K. Hayashi, Y. Okabe, N. Takeda and H. Takeya, Development of the onboard FBG demodulator for the real-time strain measurement on the composite LH_2 tank mounted on the RVT, *Proc. 8th Japan Inter. SAMPE Symp.*, 213-216 (2003).
23. H. Tamaue, J. Kuwahara, Y. Okabe and N. Takeda, Real-time detection of the dynamic behavior of CFRP laminates using small-diameter optical fiber sensors, *Proc. 8th Japan Inter. SAMPE Symp.*, 217-220 (2003).
24. T. Ogisu, M. Shimanuki, S. Kiyoshima, Y. Okabe and N. Takeda, Development of damage monitoring system for aircraft structure using a PZT actuator/FBG sensor hybrid system, *Proc. SPIE*, Vol. 5388, 427-436 (2004).